

D.K. Eskermessov¹, S.A. Pazylbek², A.K. Tussupbekova³

¹D. Serikbayev East Kazakhstan State Technical University, Ust-Kamenogorsk, Kazakhstan;

²L.N. Gumilyov Eurasian National University, Astana, Kazakhstan;

³Ye.A. Buketov Karaganda State University, Kazakhstan

(E-mail: aintus_070482@mail.ru)

Mechanical and tribological characteristics of multicomponent nitride coverings on the basis of Zr, Ti, Nb, Cr and Si

The multi-component nitride coverings on the basis of (Zr-Ti-Nb)N, (Zr-Ti-Cr-Nb)N and (Zr-Ti-Cr-Nb-Si)N are received by the method of vacuum-arc deposition from multielement cathodes Zr-Ti-Nb, Zr-Ti-Cr-Nb, Zr-Ti-Cr-Nb-Si in the environment of nitrogen (N₂). The researches show that chemical composition, microstructure and mechanical and tribological characteristics of coverings are intimately bound to deposition parameters, in particular as: pressure of working gas and potential of shift on the substrate. It is defined that multi-component coverings (Zr-Ti-Cr-Nb-Si)N and (Zr-Ti-Nb)N are simple face-centered cubic solid solution (FCC). For coverings without Si the structure generally consists of the phase TiN (FCC) and trigonal modification Cr₂N. The values of hardness were in the range (24–45 GPa). The coverings (Zr-Ti-Nb)N and (Zr-Ti-Cr-Nb) of N provide the best adhesion strength in various conditions of a sliding friction. The coverings (Zr-Ti-Cr-Nb-Si)N showed the worst adhesion strength that is possible to explain with the relative low hardness. The data of coverings are submitted perspective as protective for couples of sliding friction and cutting instrument.

Keywords: nitrides, vacuum deposition, hardness, adhesion, microstructure.

Introduction

Development of protective nitride coverings, in other words, undergoes several various stages. The first is a classical strategy of doping which mainly has one basic element for requirements of primary property and alloying additives and for secondary properties (less than 5 at. %) [1, 2]. However, the lack of these alloys is the limit of amount of suitable alloys which can be made on the required characteristics of properties. The second stage is the development of the complex ternary and quaternary nitride covering attracting the considerable scientific and production interest because of the unique combination of structural characteristics and exclusive mechanical characteristics [3–7].

For receiving the coverings meeting the rigid conditions of high performance and functionality the alloys with high entropy (HEA) were offered [8, 9]. In the HEA system there are five or more elements in equimolar ratio, and the concentration is between 5 and 35 at % for each element. It is well known that HEAs tend to form the simple FCC-and/or OCC-type of phase of solid solutions applicable to their high mixing entropy. The effects of high entropy mean that formation of random solid solutions is provided by means of contribution increase of configurational entropy to the mixing entropy because of increase in the composing elements. According to the Boltzmann dependence with the increasing mixed entropy, the free energy of interfusing accepts the lowest values which make solid solutions more stable, especially at the increasing temperatures.

This article describes primary attempts of the analysis of phase stability of nitride coverings with various quantity of the composing elements which will result in more deep comprehension of the composite interrelation between a microstructure and mechanical characteristics of multicomponent coverings. It should be noted that binary nitrides like TiN, CrN, ZrN, NbN and VN have structure FCC whereas AlN, Si₃N₄ and BN: hexagonal or amorphous [10, 11]. The formation of simple structure shows that non-FCC binary nitrides are dissolved in FCC nitrides. The presence of elements of alloy in TiN-matrix, such as Cr, improves the resistance to oxidation, Zr makes its contribution to the best wear resistance while Si and Nb increases hardness and thermal stability.

In other words, the multi-element solid solution containing the elements from the next groups of various period, such as Ti group (Ti, Zr), Nb and Cr, leads to strongly distorted lattice because of essential differences in the atomic size that considerably influence the structure and properties of these alloys.

In this research the main attention is paid mechanical and tribological properties of threefold and multi-component nitride coverings (Zr-Ti-Nb)N, (Zr-Ti-Nb-Cr) N and (Zr-Ti-Nb-Cr-Si) N received by the vacu-

um-arc deposition. The purpose is the comprehension of influence of small additives of Cr and Si elements and parameters of deposition (the negative potential the shift of the substrate and pressure of working gas) on physical mechanical and tribological properties of coverings.

Methods of experiment

The coverings (Zr-Ti-Nb)N, (Zr-Ti-Cr-Nb) N and (Zr-Ti-Cr-Nb-Si) N were deposited on the polished rotating substrate (material-steel 12X18H9T, A 570 Grade 36 steel and Si) by means of the vacuum-arc deposition, applying vacuum-arc installation «Bulat-6». Volatilized materials represented all-cast Zr-Ti-Nb cathodes (Zr — 35 at %, Nb — 35 at %, Ti — 30 at %), Zr-Ti-Cr-Nb (Cr — 37.39 at %, Zr — 27.99 at %, Nb — 22.30 at %, Ti — 12.32 at %) and Zr-Ti-Cr-Nb-Si (Cr — 17.08 at %, Zr — 30.19 at %, Nb — 9.67 at %, Ti — 39.96 at %, Si — 3.1 at %). Cathodes were manufactured by electron beam melting. The deposited (Zr-Ti-Nb)N, (Zr-Ti-Cr-Nb)N and (Zr-Ti-Cr-Nb-Si)N of the covering were performed in molecular N₂ atmosphere, pressure of working gas changed from 0.05 to 0.7 Pa. The shift of the substrate was chosen as the controlling parameter which varied from –100 to –200 V. The substrates were warmed up to 450 °C before the deposition. The distance between substrates and the cathode was 250 mm. The thickness of coverings (Zr-Ti-Nb)N and (Zr-Ti-Cr-Nb)N is 4 and 6.2÷6.8 micron respectively. The parameters of the deposition coverings (Zr-Ti-Nb)N, (Zr-Ti-Cr-Nb)N and (Zr-Ti-Cr-Nb-Si)N are presented in Table 1.

Table 1

Technological parameters of the deposition of coverings (Zr-Ti-Nb)N, (Zr-Ti-Cr-Nb)N and (Zr-Ti-Cr-Nb-Si)N

Series No.	Precipitated material	Arc current I_{arc} , A	Nitrogen pressure P_N , Pa	Bias voltage U_{bias} , V
1	(Zr-Ti-Nb)N	95	0.05	–100
2			0.5	–100
1	(Zr-Ti-Cr-Nb)N	110	0.3	–100
2			0.7	–100
3			0.3	–200
4			0.7	–200
1	(Zr-Ti-Cr-Nb-Si)N	110	0.3	–100
2			0.3	–200

The chemical composition and morphology of coverings were investigated with use of the X-ray power dispersion spectrometer PEGASUS system, the scanning submicroscopy / power dispersion X-ray spectroscopy (SEM/EDX) JEOL JSM-6610 LV and JEOL 7001TTLS with the voltage 15–20 kV.

The research of mechanical characteristics of the nitride coverings deposited at various parameters of deposition was carried out by means of microhardness gages DM8-B and Durascan-20» produced of the «CSM Systems AG company» (Switzerland). The prints were made at the distance 1.0 mm from each other, for each exemplar ten measurements were taken. To reduce influence of dropwise component, the coating surfaces were polished after the deposition. Nanohardness and elastic modulus measured with use of nanodimpling (Hysitron TI 950 TriboIndenter) with the diamond indenter Berkovich, the maximum load made 10000 mkN. The values of hardness and elastic modulus on loading unloading curves with use of the Oliver-Farrah method were measured.

For measurement of adhesion of coverings (Zr-Ti-Nb)N, (Zr-Ti-Cr-Nb)N and (Zr-Ti-Cr-Nb-Si)N, the scratch-tester REVETEST equipped with a diamond indenter of Rockwell C with a radius of curving of 200 mm was used. For obtaining reliable results two scratches on coating surfaces were made. The morphology of the track surface was traced by means of the optical and scanning supermicroscope FEI NovaNanoSEM 450. The following main ultimate loads on change of graphs of the friction coefficient and acoustic emission from scratching loading — L_C were fixed.

The tribological tests were carried out by the automated car of sliding friction «Tribometer» brand in the open air according to the scheme «ball-disk» at the temperature 20 °C. The disks on which coverings were applied were made of steel 45 (HRC = 55) with the diameter 42 mm, 5 mm high. As a counterbody the ball with the diameter 6.0 mm made from the baked certified material — Al₂O₃ was used. The loading made 3.0 N, sliding speed 10 cm/sec.

Results and discussion

The results of mechanical characteristics, in particular, hardness of all received coverings, are given in Table 2.

Table 2

Mean values of hardness of nitride coverings

Covering	Series	Hardness, GPa
(Zr-Ti-Nb)N HV _{0,05}	1	37.2
	2	44.5
(Zr-Ti-Cr-Nb)N HV _{0,1}	1	30.9
	2	34.7
	3	38.8
	4	43.9

Apparently from Table 2, the maximal value of hardness (44.5 GPa) for nitride covering (Zr-Ti-Nb)N is reached with the pressure of reactionary $P_N=0,5$ Pa. As we see, the hardness of coverings (Zr-Ti-Cr-Nb)N deposited at $P_N=0,3$ Pa and $U=-100$ V is 30.9 GPa and changes up to 38.8 GPa at increase in potential of shift on the substrate up to -200 V. It should be noted that the coverings put at lower content of nitrogen have low hardness. When P_N increases up to 0.7 Pa, the hardness increase is explained by formations of larger number of the strong connections of Me/N which are present in films. Besides, high hardness can be caused by the high content of the phase Cr_2N as hardness of the covering Cr_2N is higher, than CrN covering.

For nitride coverings (Zr-Ti-Cr-Nb-Si)N deposited at $P_N=0.3$ Pa and $U=-100$ V, the hardness is 29 GPa, and the elastic modulus makes 291 GPa. With increase in shift potential on the substrate up to -200 V the hardness and elastic modulus respectively decreased up to 24 and 254 GPa. One of explanations of decrease in hardness is excessive ionic bombing therefore coverings become less textured, transition from mainly (111) orientation with high intensity to the content of FCC-orientation, including additional orientations (111) and (200).

Nanohardness and elastic modulus of coverings (Zr-Ti-Cr-Nb-Si)N were measured with use of the nanoindenter «Hysitron TI 950 TriboIndenter» with the Berkovich diamond indenter, the maximum load made 10000 mcN. We estimated the value of hardness and elastic modulus from indenter loading unloading curves by means of the Oliver and Farrah methods. From tests of nanoindenting of loading-unloading of curve coverings (Zr-Ti-Cr-Nb-Si)N, nanohardness and elastic modulus of the films deposited on the substrate at various shift potentials were defined and shown in Figure 1.

The test data on adhesion of coverings (Zr-Ti-Nb)N, (Zr-Ti-Cr-Nb-Si)N and (Zr-Ti-Cr-Nb)N received at various technological parameters of deposition are provided in Table 3. The research results of adhesion-cohesive strength and resistance of coverings to scratching are given in Figures 2 and 3. The reference values of ultimate load L_C were determined by change of values of friction coefficient and signal of acoustic emission at increase in loading of scribing: L_{C1} — emergence of the first chevron crack at the bottom and diagonal crack at the edges of scratch; L_{C2} — formation of multiple cracks at the bottom of scratch and local peeling of the covering, formation the chevron cracks at the bottom of scratch; L_{C3} — cohesive-adhesion failure of the covering; L_{C4} — ductile attrition of the covering. As a criterion of the adhesion strength the value of ultimate loading L_{C4} when there is covering attrition was accepted.

According to these criteria, the process of destruction of covering when scratching by the indenter can be divided into four stages conditionally. In the range of loadings from $F=0.9$ to 9.89 N there is the monotonic penetration of the indenter into the covering, at the same time the friction coefficient slightly increases, and the signal of acoustic emission remains unchanged. At $F=15.81$ N loading the indenter completely plunges into the covering, and sliding of the diamond indenter on the covering happens with the friction coefficient 0.35. When increase in loading ($F=20.6-36.4$ N) there is the expression of material before the indenter in the form of pimples and increase in depth of indenter penetration.

The comparative analysis shows that coverings (Zr-Ti-Cr-Nb)N are erased, but they do not exfoliate during scratches, i.e. they collapse thanks to the cohesive mechanism of plastic deformation and fatigue cracking in material of coverings. In Figure 4 the curve of the friction coefficient change is shown (μ) when moving the diamond indenter of coating surfaces of the system (Zr-Ti-Cr-Nb)N (exemplar 4), change curve

of acoustic emission (AE) and the image of the remained covering fragments at the bottom of scratch after influence of the diamond indenter.

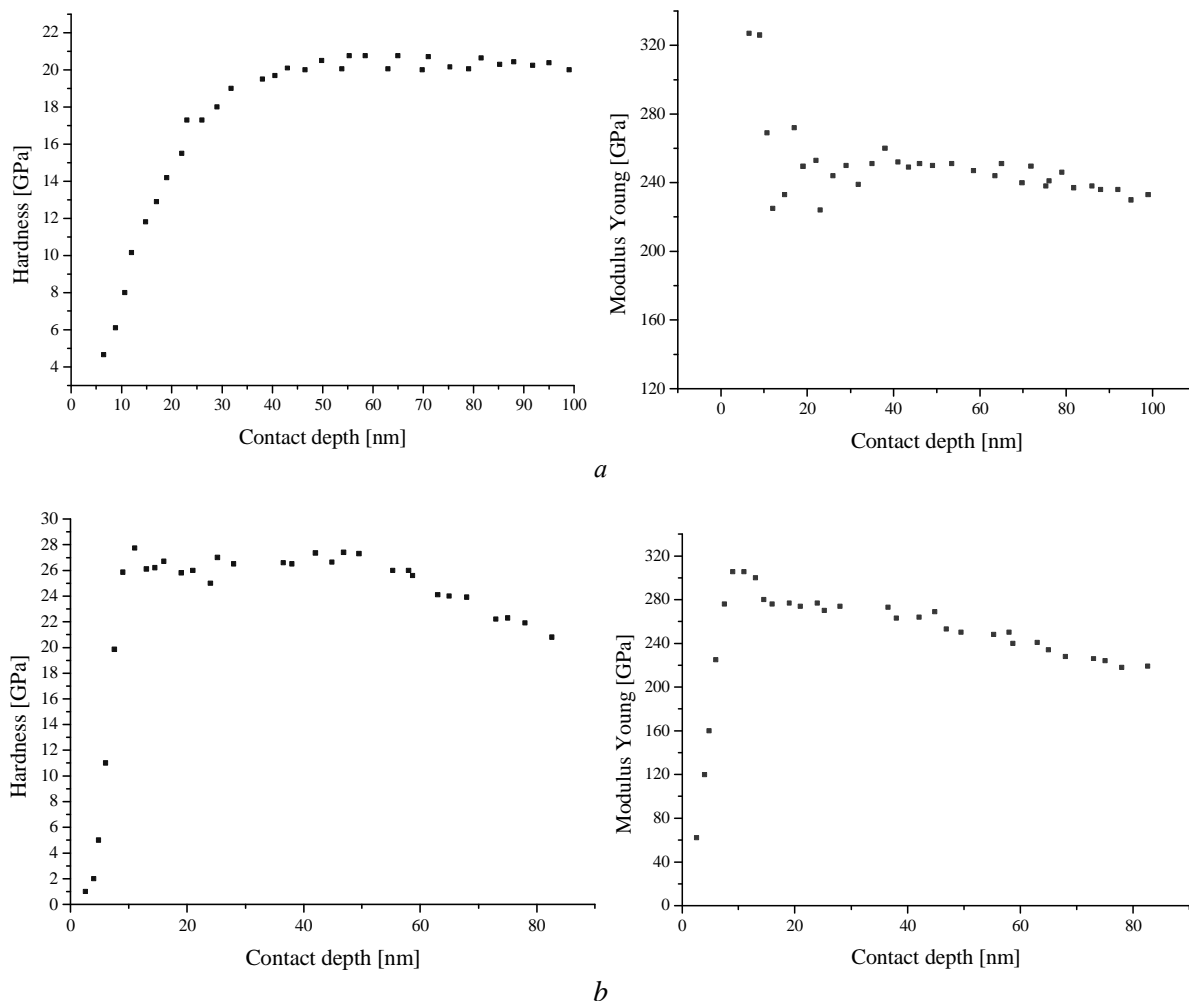


Figure 1. Dependences of hardness and elastic modulus on contact depth for coverings (Zr-Ti-Vr-Nb-Si)N, at $P_N = 0.3$ Pa and different values U –100 V (a), –200 V (b)

Table 3

Comparative results of the adhesion tests for coverings (Zr-Ti-Nb)N, (Zr-Ti-Cr-Nb)N and (Zr-Ti-Cr-Nb-Si)N

Covering	Critical loads [N]	Series No.			
		1	2	3	4
(Zr-Ti-Nb)N	L_{C1}	2.91	9.89	–	–
	L_{C2}	29.04	20.62	–	–
	L_{C3}	43.18	36.43	–	–
	L_{C4} (L_{C5})	59.26	66.77	–	–
(Zr-Ti-Cr-Nb)N	L_{C1}	10.94	11.8	10.35	15.21
	L_{C2}	18.69	20.93	18.42	24.29
	L_{C3}	26.95	30.35	23.12	33.45
	L_{C4}	39.15	45.94	45.12	40.97
	L_{C5}	49.09	56.17	61.08	62.06
(Zr-Ti-Cr-Nb-Si)N	L_{C1}	9.54	11.28	–	–
	L_{C2}	12.48	14.04	–	–
	L_{C3}	18.36	24	–	–
	L_{C4}	29.86	34.09	–	–
	L_{C5}	45.33	45.57	–	–

As we see, the monotonic penetration of the indenter into the covering takes place, and the first cracks appear (loading up to 15.21 N); the friction coefficient (μ) increases, but the signal of acoustic emission remains invariable. Further, when increase in loading there is emergence of chevron and diagonal cracks that leads to increase in the friction coefficient up to the value 0.3.

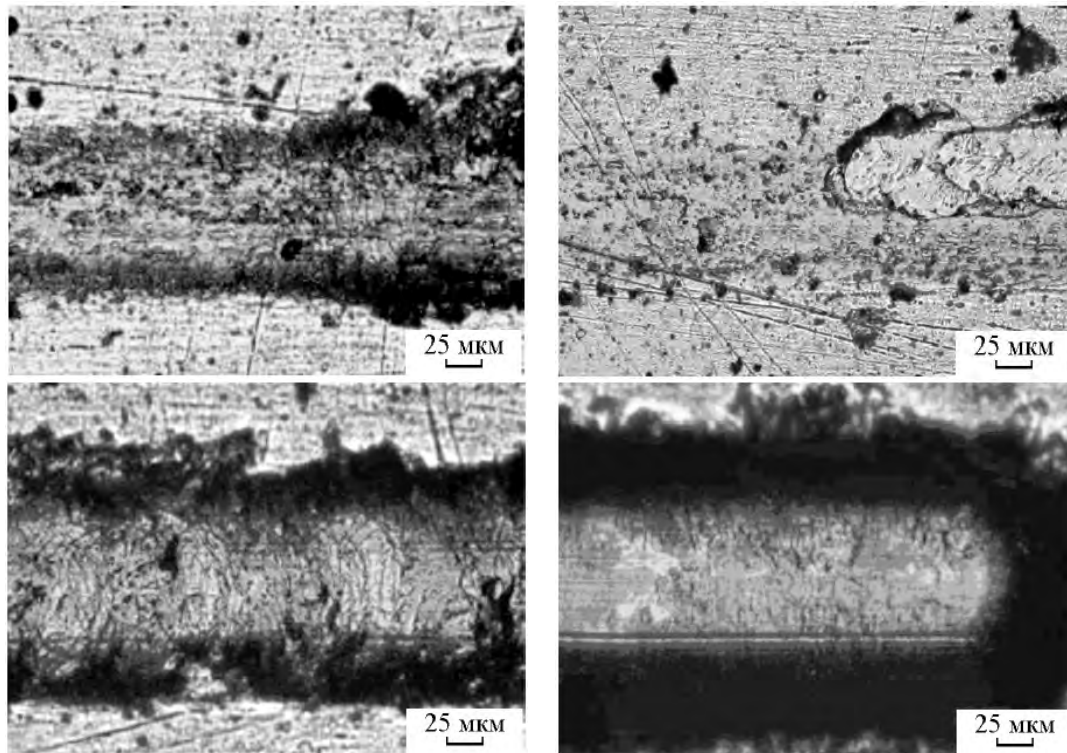


Figure 2. Microphotographs of the contact area of the diamond indenter with a covering (Zr-Ti-Nb)N ($P_N = 0.5$ Pa), at different stages of scratch-testing

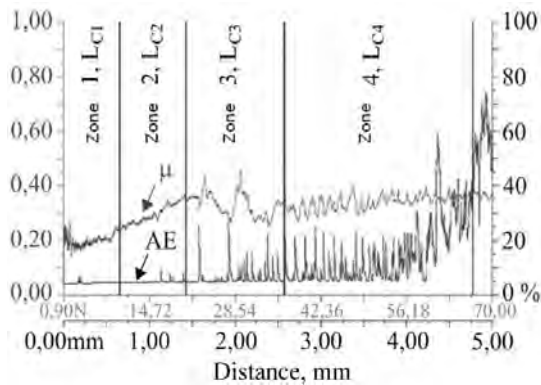


Figure 3. Dependence of the friction coefficient and signal of acoustic emission from applied load at scratch-testing of the covering (Zr-Ti-Nb)N, received at $P_N = 0.5$ Pa

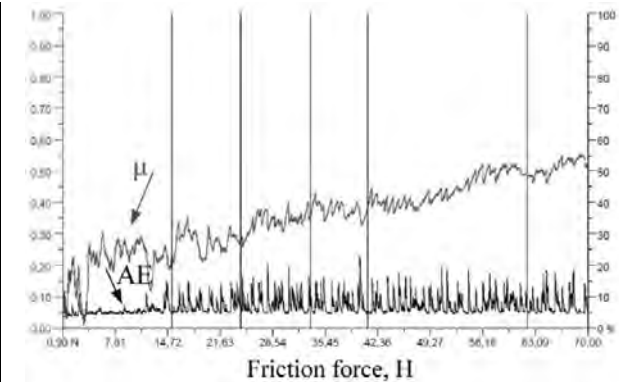


Figure 4. Dependence of the friction coefficient and signal of acoustic emission from applied load at scratch-testing of the covering (Zr-Ti-Cr-Nb)N (series 4)

When loading up to 14 N the amplitude of signal of acoustic emission sharply increases, and its value remains at the same level until the end of the test. After that, when increase in loading up to 62 N, there is local attrition of the covering down to the substrate material.

The dependence of the friction coefficient change and acoustic emission on the applied load on exemplars of the covering (Zr-Ti-Cr-Nb-Si)N, for series 1 and 2 is shown in Figure 5. As we see, at load of 9 N (L_{C1} for series 1) and 11 N (L_{C1} for series 2) correspond to emergence of the first cracks and scraps (Fig. 6 and 7). It is confirmed by the beginning of the increase of amplitude of acoustic emission (Fig. 5). The initial attrition of coverings occurs at loadings $L_{C3}=18$ N (series 1) and $L_{C3}=24$ N (series 2) (Fig. 6 and 7) that leads

to increase in the friction coefficient up to value 0.49 for all coverings. The local attrition of coverings to the material of the substrate occurs when loading reaches values 45 and 46 N. In this case, the friction coefficient increases up to the maximal value 0.63.

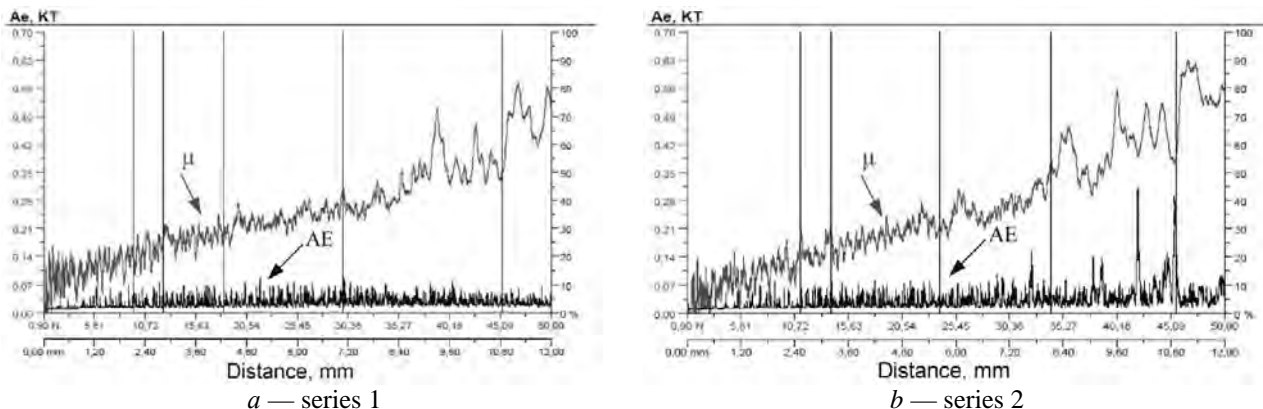
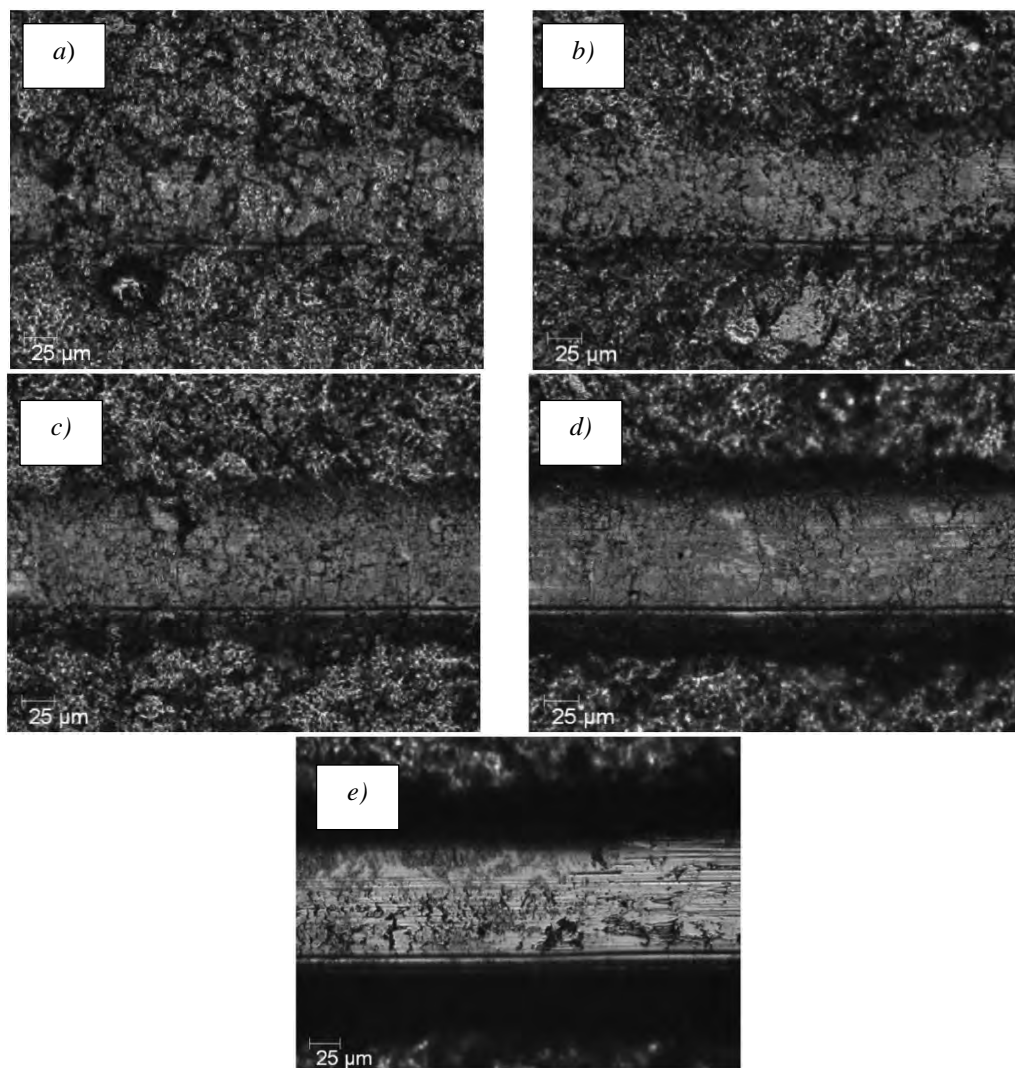
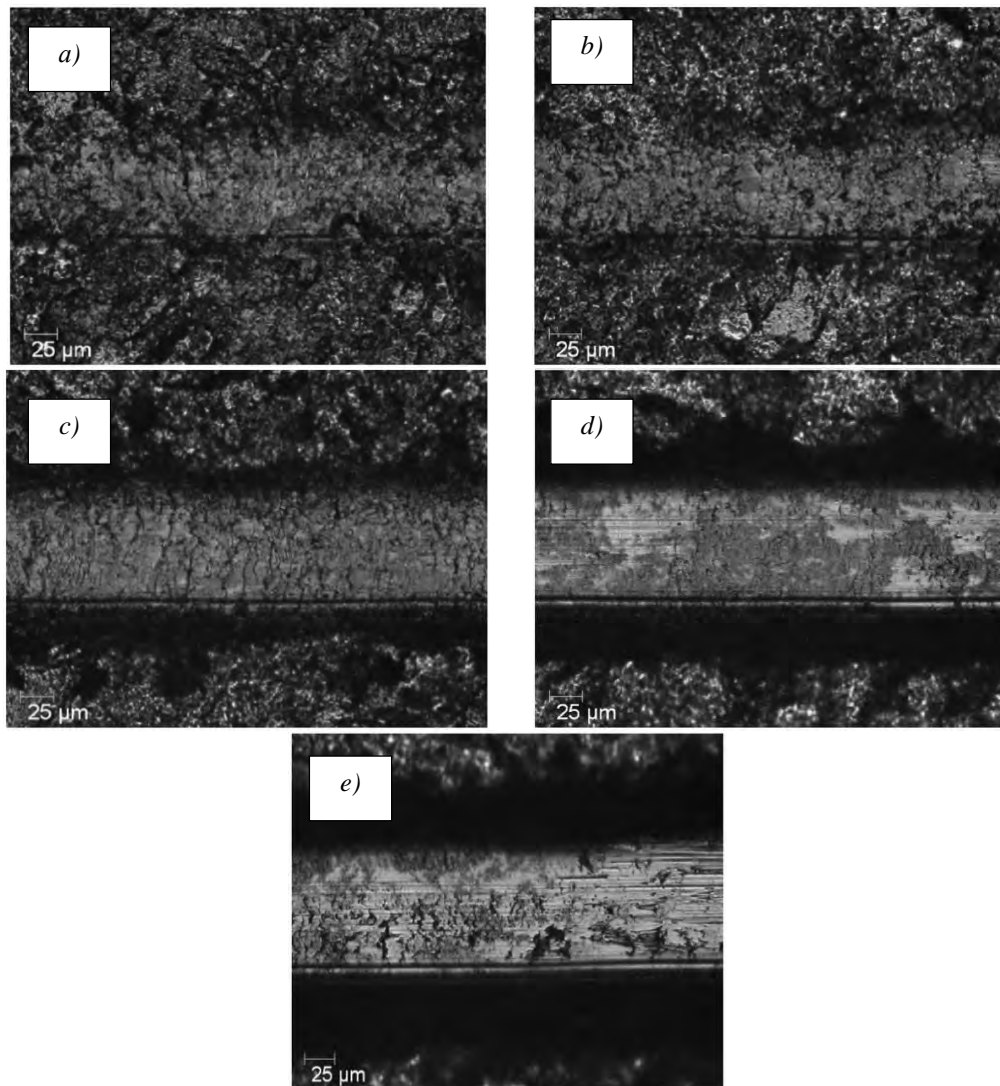


Figure 5. Dependence of the friction coefficient and signal of acoustic emission on the applied load when scratch-testing of the covering (Zr-Ti-Cr-Nb-Si)N



a — 9.54 N (L_{C1}); b — 12.48 N (L_{C2}); c — 18.36 N (L_{C3}); d — 29.86 N (L_{C4}); e — 45.33 N (L_{C5})

Figure 6. Microphotographs of the contact area of the diamond indenter with the covering (Zr-Ti-Cr-Nb-Si)N (series 1), at different loads of the indenter



a — 11.28 N (L_{C1}); *b* — 14.04 N (L_{C2}); *c* — 24 N (L_{C3}); *d* — of 34.09 N (L_{C4}); *e* — 45.57 N (L_{C5})

Figure 7. Microphotographs of contact area of the diamond indenter with covering (Zr-Ti-Cr-Nb-Si)N (series 2), at different loads of the indenter

For multicomponent coverings (Zr-Ti-Cr-Nb-Si)N for series 1 the adhesion durability at different intervals of the experiment significantly differs from durability of coverings (exemplars) of series 2. With increase in loading, noticeable distribution of crack on coating surfaces does not happen.

Based on the nature of destruction, the main contribution, apparently, is connected to shear stresses. Cohesion failure arises at cracking fissuring in the plane, perpendicular to the direction of the covering growth. The first signs of attrition of covering were written down at loading 18 N.

In Figure 8 the changes of chemical composition of coverings (Zr-Ti-Cr-Nb-Si)N are shown during the scratching test (scratch-test). Sharp increase in concentration of iron (at the distance 3 mm) corresponds to the emergence of the first cracks and the beginning of tentative attrition of coverings.

Besides, it should be noted that the content of iron in the covering increases more intensively, at the shift potential $U_{CM} = -100$ V. This statement is confirmed by lower value of ultimate load (18.36 and 24 N respectively) that corresponds to the beginning of tentative attrition of coverings (see Table 3). Chemical composition of coverings (Zr-Ti-Cr-Nb-Si)N at the local attrition are almost identical, but concentration of nitrogen of series 2 is higher, than in series 1 that will be coordinated with the result EDX.

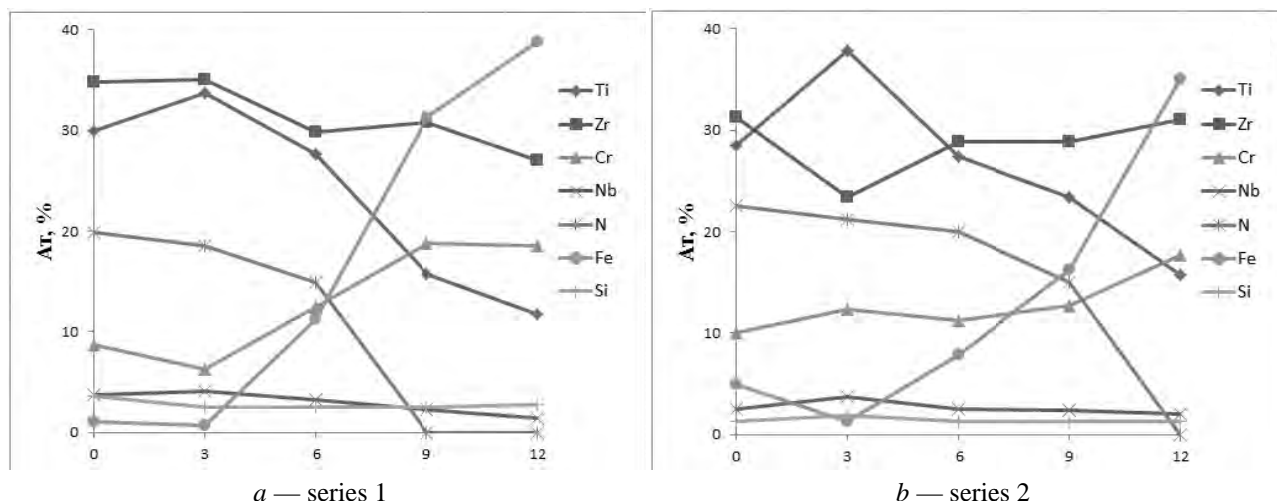


Figure 8. Chemical composition of coverings of scratch after test

Test data on the adhesion strength show that coverings were worn-out during scratches, but did not exfoliate, that is destruction happened at the expense of the cohesive mechanism, connected to the plastic strain and fatigue cracks in covering material.

The comparative analysis shows (see Table 3) that the difference in anchoring strength (adhesion) of coverings, is apparently caused by differences in their structure and mechanical characteristics.

As it is shown in Table 3, with increase in shift of the substrate the adhesion strength between the covering and the substrate increases. The increased adhesion can be connected to the increased stability of fracturing and plastic strain. Loadings (L_{C5}) for coverings (Zr-Ti-Cr-Nb)N and (Zr-Ti-Cr-Nb-Si)N increase with increase in shift of the substrate (from -100 to -200 V) their maximal value made 62.06 and 45.57 N respectively. Besides, it should be noted that coverings, received at high potential of the shifts, have higher hardness, and are steadier [12, 13]. Nitride coverings (Zr-Ti-Cr-Nb) N and (Zr-Ti-Cr-Nb-Si)N with a good adhesion strength show high values of hardness of 43.9 and 27.5 GPa respectively. Comparing results from tables 2 and 3, it is possible to see that coverings with a high hardness possess good adhesion strength.

As it is shown in Figure 9, the covering has the homogeneous surface with minimum inclusion of macroscopic particles. The presence of small craters is apparently connected to processes of dispersion because of high energy of the sraid ions.

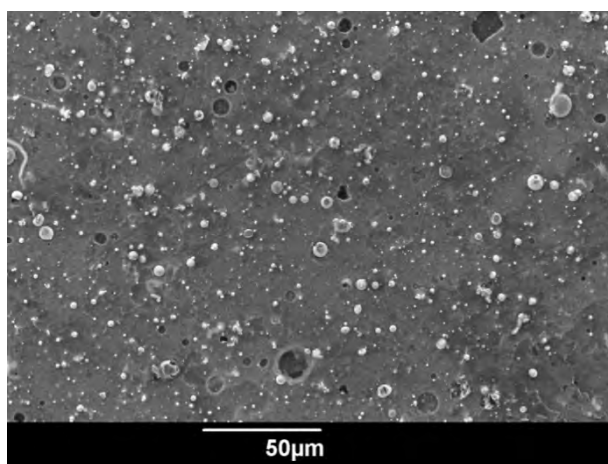


Figure 9. Morphology of nitride covering (Zr-Ti-Nb)N, received at $U_{cm} = -200$ V and $P_N = 0.5$ Pa

Profilogramm of surfaces of steel disk before and after test are given in Figures 10 and 11.

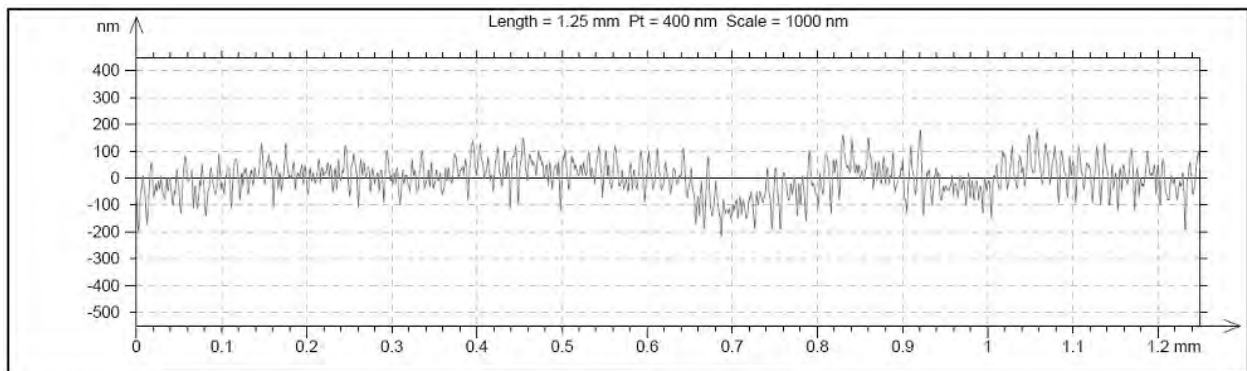


Figure 10. Profile of surface roughness of steel disk after polishing

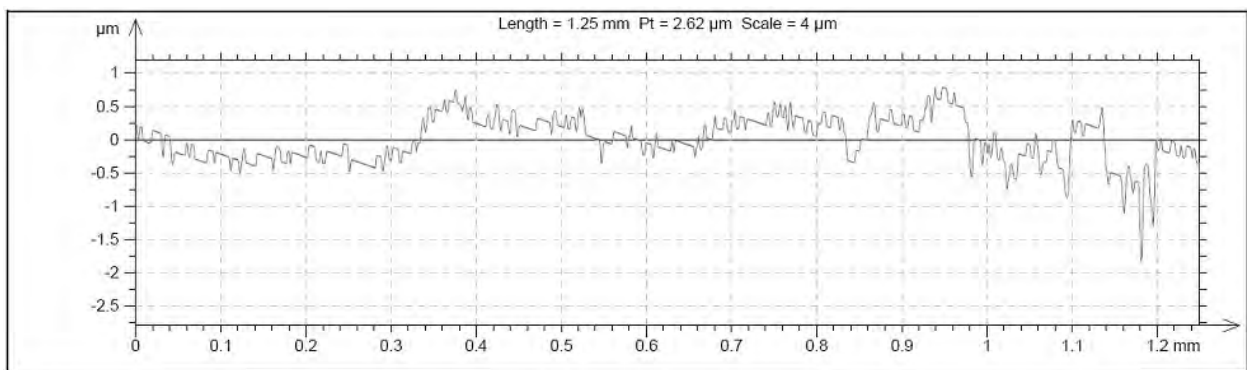


Figure 11. Profile of surface roughness of steel disk after deposition (Zr-Ti-Nb)N

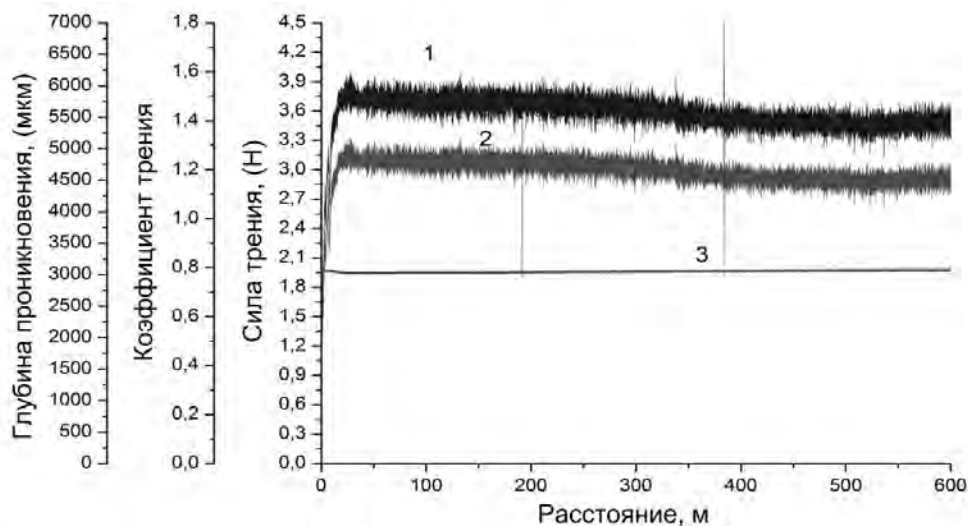


Figure 12. Results of tribological tests of steel disk after deposition (Zr-Ti-Nb)N

At absence of covering the roughness of the disk is $R_a = 0.088$ microns. The covering (Zr-Ti-Nb)N (thickness is about 4.0 microns) in the environment of reactionary gas of nitrogen by the method of vacuum-arc deposition on the polished surface of steel disk leads to increase in roughness (Fig. 11) up to 0.42 microns.

The noticeable increase in roughness of steel disk is, apparently, connected both to existence of the stream of macroscopic particles and to formation of craters when deposition of covering. Results of

tribological tests of steel disk after deposition are presented in Figure 12 and in Table 4. The important parameter defining operability of the covering are also its tribological characteristics (friction coefficient and wear factor). The friction coefficient μ defines the cohesive force of the rubbing materials, and wear factor — resistance to wear (the wear factor is less, the wear resistance is higher).

Table 4

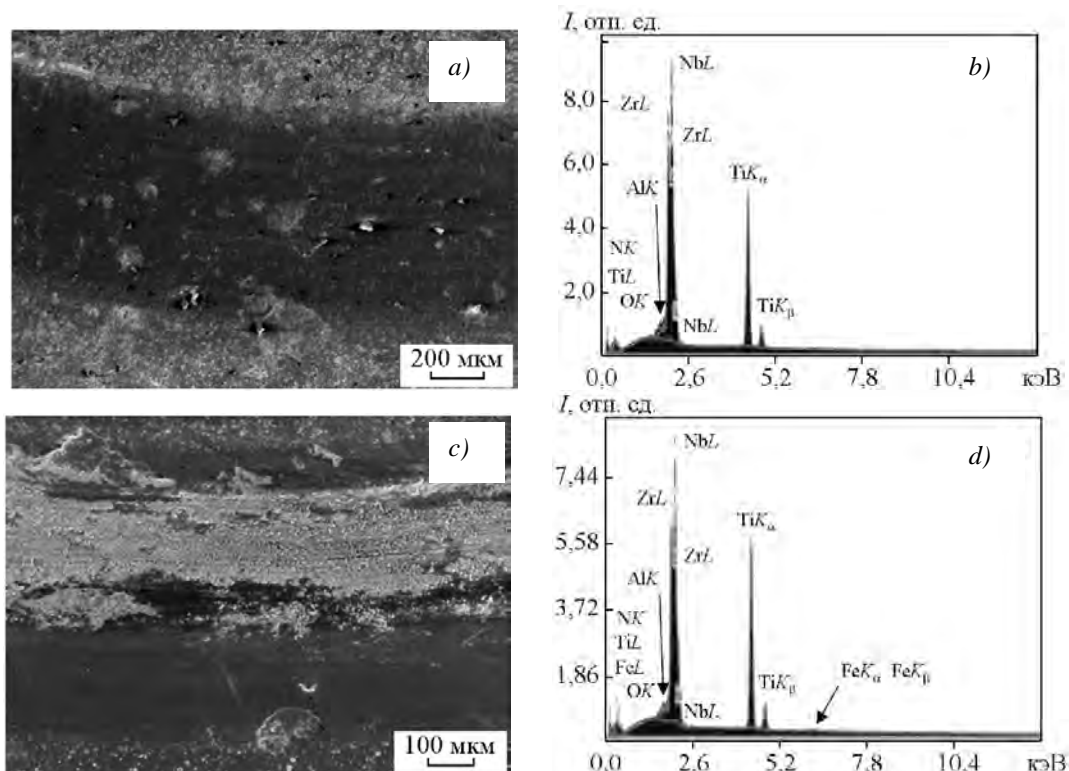
Tribological characteristics of the «covering (Zr-Ti-Nb)N — Al₂O₃» system

Cover (Zr-Ti-Nb)N, series	Coefficient of friction μ		Wear factor $W, 10^{-5} \text{ mm}^3/\text{N}\cdot\text{m}$	
	Initial value	Value during testing	Counter	Coated sample
1	0.61	1.95	0.391	9.69
2	0.491	1.05	3.21	2.4
Steel 45 (substrate)	0.204	0.674	0.269	35.36

From the data presented in Figure 11 and in Table 4 it is clear that drawing the nitride covering (Zr-Ti-Nb)N on the steel 45 leads to increase in the friction coefficient from 0.674 to 1.95 that will be coordinated with results of research of surface roughness of the steel disk.

The friction coefficient accepts the values from initial (during the first contact), to stationary (column «while tests» in Table 4) — when exit to constant values while tests.

On all exemplars with covering (series 1, 2) the friction coefficient appeared higher than 1.0. So high values can be explained with high roughness (Fig. 9), connected to existence of the dropwise fraction which is formed when vacuum-arc deposition both on the surface and covering. Emergence of solid dropwise component as well as formation of wear products in the form of the particles consisting of solid nitrides when destruction of the covering leads to abrasive wear of the covering. Decrease of roughness reduces a friction coefficient from 1.95 to 1.05. With increase in covering hardness (see Table 2) the wear factor W of the coverings decrease, but if counterbodies — it increases (Table 4).



a, b — series 1 exemplar; *c, d* — series 2 exemplar

Figure 13. Coating surfaces of system (Zr-Ti-Nb)N after tribotechnical tests (*a, c*) and power dispersion ranges of paths of the sliding friction (*b, d*)

The research of paths of sliding friction as a result of which it is possible to draw the conclusion on the wear mechanism is of the considerable interest. It is known that the main mechanisms of covering wear when sliding friction are: 1) the adhesion wear at which there is covering material sticking to the counterbody; 2) abrasive wear when there is formation by more solid material of the counterbody of grooves on the surface of material; 3) fatigue wear — process of removal of covering particles; 4) plastic strain of material of covering.

Photos of paths of sliding friction of the covering (Zr-Ti-Nb)N received by the method of vacuum-arc deposition are provided in Figure 13 (*a* and *c*). Analyzing images of sliding friction paths of the studied covering, it is possible to draw the conclusion that existence of signs of scratches and also wear of similar products particles (Fig. 13) demonstrate the abrasive nature of covering wear. From the provided drawings (Fig. 12) it is visible that the flute has a smooth surface. The existence of the similar flute is apparently connected to a large amount of defects in the covering.

Results of the analysis of wear products along the created flute are given in Figure 13 (*b* and *d*). From the micrograph of wear products the counterbody material availability clearly is visible on the surface.

The energy dispersion range (Fig. 13, *b* and *d*) demonstrates to aluminum oxide availability on coating surfaces that is, apparently, connected to counterbody material transfer. This circumstance is confirmed by the data presented in Table 4 namely by comparison of factors of counterbody wear and the studied exemplar.

Results of profilogramm processing demonstrate that mean value of the substrate roughness for the deposited coverings (Zr-Ti-Cr-Nb)N makes micron $R_a=0.089$, and it changes after the deposition of the covering (Fig. 14). ASM-images of the topography of coating surfaces of 4-series of system (Zr-Ti-Cr-Nb)N are provided in Figure 15.

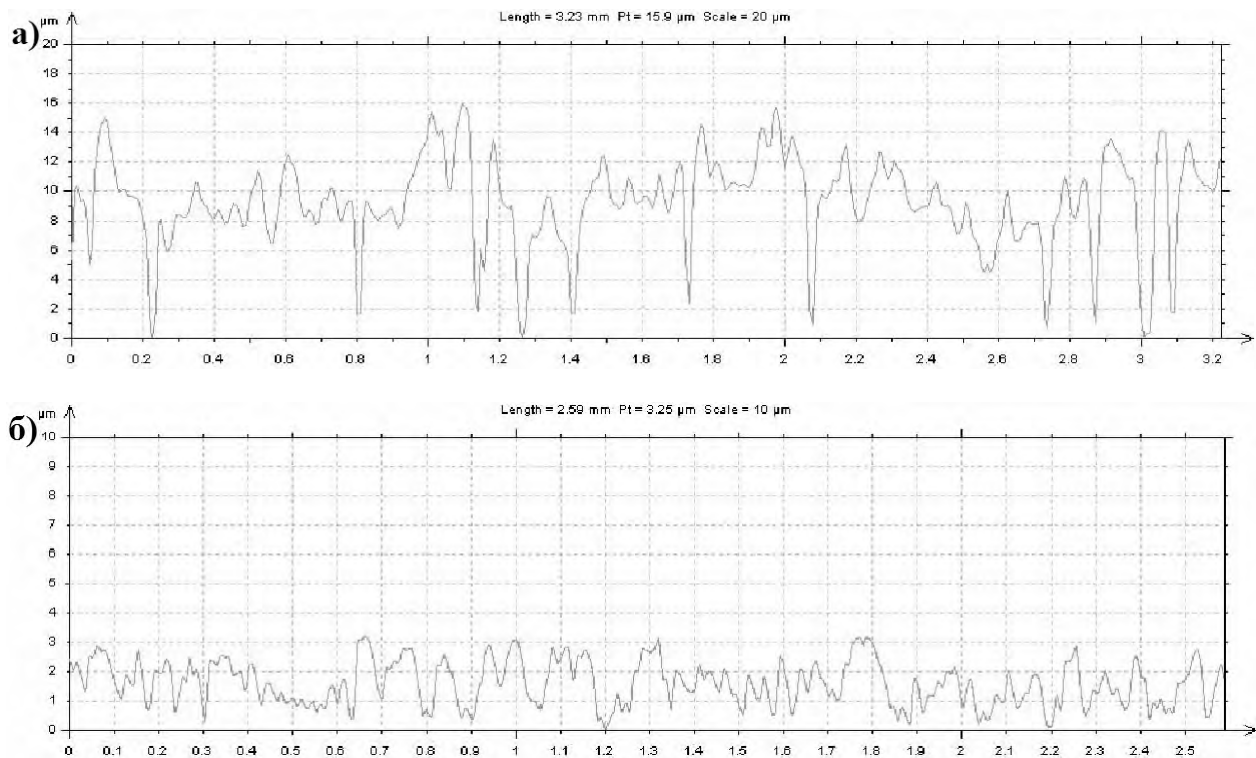
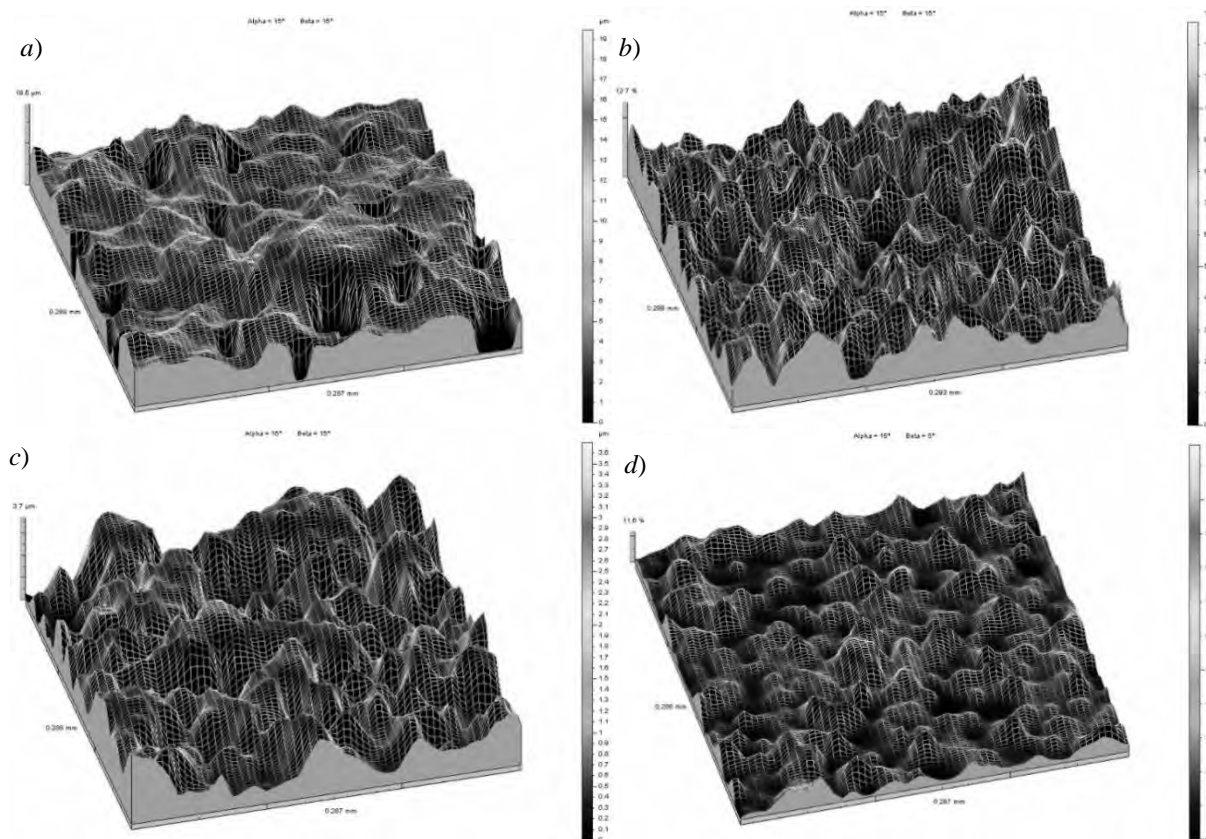


Figure 14. Profile of surface roughness of coverings (Zr-Ti-Cr-Nb)N of the series 1 (*a*) and series 4 (*b*)

Comparison of the obtained data shows that roughness change (Zr-Ti-Cr-Nb)N directly depends on the pressure of reactionary gas of nitrogen and potential of mixture. At the pressure $P_N = 0.7$ the coating surfaces turn out more homogeneous, with obviously expressed dropwise inclusions of the small sizes. At the pressure $P_N = 0.3$ Pa on coating surfaces not completely melted compounds of the elements Ti, Zr, Cr, Nb, with nitrogen are formed.



a — $P_N = 0.3$ Pa, $U_b = -100$ V, $R_a = 1,69$ mm (series 1); *b* — $P_N = 0.7$ Pa, $U_b = -100$ V, $R_a = 1,83$ mm (series 2);
c — $P_N = 0.3$ Pa, $U_b = -200$ V, $R_a = 1,88$ mm (series 3); *d* — $P_N = 0.7$ Pa, $U_b = -200$ V, $R_a = 1,55$ mm (series 4)

Figure 15. ASM three-dimensional image of coating surfaces (Zr-Ti-Cr-Nb)N

Conclusions

The role of Cr and Si additives to properties of coverings (Zr-Ti-Nb)N, including structure and the relative hardness is investigated. The research results were generalized as follows:

1. The interrelation of structural and phase state and mechanical characteristics of coverings is investigated. It is established that hardness of nitride coverings (Zr-Ti-Nb)N depending on physical properties of the deposition varies from 37.2 to 44.5 GPa.

2. The analysis of experiments concerning measurement of microhardness indicates that hardness for coverings (Zr-Ti-Cr-Nb)N depending on physical properties of the deposition is in range from 30.9 to 43.9 GPa.

3. The influence of physical technological parameters of the deposition on hardness and the elastic modulus for nitride coverings (Zr-Ti-Cr-Nb-Si)N deposited at $P_N = 0.3$ Pa and $U = -100$ V is investigated, hardness is 29 GPa, and the elastic modulus makes 291 GPa.

4. It is shown that drawing the covering (Zr-Ti-Nb)N on the steel disk leads to increase in a friction coefficient from 0.674 to 1.95. The wear resistance research (wear factor) of the analyzed covering showed noticeable increase in resistance of the exemplar to wear ($0.039 \cdot 10^{-5} \text{ H}^{-1} \cdot \text{mm}^{-1}$ and $35.36 \cdot 10^{-5} \text{ mm}^3 \cdot \text{H}^{-1} \cdot \text{mm}^{-1}$).

5. It was revealed that the adhesion of the studied coverings was improved due to use of higher parameters of the deposition (potential of shift and pressure of working gas of nitrogen). Local wear of coverings (Zr-Ti-Cr-Nb-Si)N to material of the substrate happens when loading reaches the greatest value of 46 N for the coverings (Zr-Ti-Cr-Nb)N — 62 N and for (Zr-Ti-Nb)N — 66 N.

References

- 1 Petrov, I., Barna, P.B., Hultman, L., & Greene, J.E. (2003). Microstructural evolution during film growth. *J. Vac. Sci. Technol. A*, 21, 117–128.
- 2 Tan, S., Zhang X., Wu, X., Fang, F., Jiang, J. (2011). Effect of substrate bias and temperature on magnetron sputtered CrSiN films. *Appl. Surf. Sci.*, 257, 1850–1853.
- 3 Pogrebnnyak, A.D., Shpak, A.P., Kirik, G.V., Erdybaeva, N.K., Il'yashenko, M.V., & Demyanenko, A.A., et al. (2011). Multilayered nano-microcomposite Ti-Al-N/TiN/Al₂O₃ coatings. Their structure and properties. *Acta Phys. Pol. A*, 120(1), 94–99.
- 4 Pogrebnnyak, A.D., Sobol, O.V., Beresnev, V.M., Turbin, P.V., Dub, S.N., & Kirik, G.V., et al. (2009). Features of the structural state and mechanical properties of ZrN and Zr(Ti)-Si-N coatings obtained by ion-plasma deposition technique. *Tech. Phys. Lett.*, 35(10), 925–928.
- 5 Sobol, O.V., Pogrebnnyak, A.D., & Beresnev, V.M. (2011). Effect of the preparation conditions on the phase composition, structure, and mechanical characteristics of vacuum-Arc Zr-Ti-Si-N coatings, *Phys. Met. Metallogr.*, 112, 188–195.
- 6 Pogrebnnyak, A.D., Ponomarev, A.G., Kolesnikov, D.A., Beresnev, V.M., Komarov, F.F., Melnik, S.S., et al. (2012). Effect of mass transfer and segregation on the formation of superhard nanostructured Ti-Hf-N(Fe) coatings. *Tech. Phys. Lett.*, 38, 623–626.
- 7 Pogrebnnyak, A.D., Postol'nyi, B.A., Kravchenko, Y.A., Shipilenko, A.P., Sobol, O.V., & Beresnev, V.M., et al. (2015). Structure and Properties of (Zr-Ti-Cr-Nb)N Multielement Superhard Coatings, *J. Superhard Mater.*, 37, 101–111.
- 8 Pogrebnnyak, A.D., Bagdasaryan, A.A., Yakushchenko, I.V., & Beresnev, V.M. (2014). The structure and properties of high-entropy alloys and nitride coatings based on them, *Rus. Chem. Rev.*, 83(11), 1027–1061.
- 9 Braic, V., Balaceanu, M., Braic, M., Vladescu, A., Panseri, S., & Russo, A. (2012). Characterization of multi-principal-element (TiZrNbHfTa)N and (TiZrNbHfTa)C coatings for biomedical applications, *J. Mech. Behav. Biomed. Mater.*, 10, 197–205.
- 10 Martin, P.J., Bendavid, A., Cairney, J.M., & Hoffman, M. (2005). Nanocomposite Ti-Si-N, Zr-Si-N, Ti-Al-Si-N, Ti-Al-V-Si-N thin film coatings deposited by vacuum arc deposition, *Surf. Coat. Technol.*, 200, 2228–2235.
- 11 Hsieh, M.H., Tsai, M.H., Shen, W.J., & Yeh, J.W. (2013). Structure and properties of two Al-Cr-Nb-Si-Ti high-entropy nitride coatings. *Surf. Coat. Technol.*, 221, 118–123.
- 12 Pogrebnnyak, A.D., Yakushchenko, I.V., Bondar, O.V., Beresnev, V.M., Oyoshi, K., & Ivasishin, O.M., et al. (2016). Irradiation resistance, microstructure and mechanical properties of nanostructured (TiZrHfVNBa)N coatings. *J. Alloy Compd.*, 679, 155–163.
- 13 Shpylenko, A., Pshyk, A.V., Grzeskowiak, B., Medyanik, K., Peplinska, B., & Oyoshi, K., et al. (2016). Effect of ion implantation on the physical and mechanical properties of Ti-Si-N multifunctional coatings for biomedical applications. *Mater. Des.*, 110, 821–829.
- 14 Pogrebnnyak, A., Maksakova, O., Kozak, C., Koltunowicz, T.N., Grankin, S., & Bondar, O. et al. (2016). Physical and mechanical properties of nanostructured (Ti-Zr-Nb)N coatings obtained by vacuum-arc deposition method. *Przegląd elektrotechniczny*, 180–183. doi: 10.15199/48.2016.08.49.
- 15 Beresnev, V.M., Sobol, O.V., Grankin, S.S., Nemchenko, U.S., Novikov, V.Yu., & Bondar, O.V. et al. (2016). Physical and mechanical properties of (Ti-Zr-Nb)N coatings fabricated by vacuum-arc deposition. *Inorganic Materials: Applied Research.*, 7, 3, 388–394. doi: 10.1134/S2075113316030047.
- 16 Plotnikov, S.V., Pogrebnnyak, A.D., Yerokhina, L.N., & Yeskermessov, D.K. (2015). Study of nanostructured (Ti-Zr-Nb)N coatings' physical-mechanical properties obtained by vacuum arc evaporation. Proceedings from RTEP2015 IOP Conf. Series: Materials Science and Engineering (p. 1–6). doi:10.1088/1757-899X/110/1/012031.
- 17 Maksakova, O.V., Grankin, S.S., Bondar, O.V., Kravchenko, Ya.O., Yeskermessov, D.K., & Prokopenko, A.V. et al. (2015). Nanostructured (Ti-Zr-Nb)N coatings obtained by vacuum-arc deposition method: structure and properties. *Journal of Nano- and Electronic Physics*, 7, 4, 1–7.
- 18 Yeskermessov, D.K., Plotnikov, S.V., & Yerdybaeva, N.K. (2016). Structure and properties of multi component (Ti-Zr-Cr-Nb)N coatings obtained by vacuum-arc deposition. *Tribologia*, 205–218.

Д.К. Ескермесов, С.А. Пазылбек, А.К. Тусупбекова

Zr, Ti, Nb, Cr және Si негізіндегі көпкомпонентті нитридті жабындардың механикалық және трибологиялық сипаттамалары

Zr-Ti-Nb, Zr-Ti-Cr-Nb және Zr-Ti-Cr-Nb-Si көпэлементті катодтардан вакуумды-доғалық тұндыру әдіспен азотты (N₂) ортада (Zr-Ti-Nb)N, (Zr-Ti-Cr-Nb)N және (Zr-Ti-Cr-Nb-Si)N негізіндегі көпкомпонентті нитридті жабындар алынды. Жүргізілген зерттеулер жабындардың химиялық құрамы, микроқұрылымы, механикалық және трибологиялық қасиеттері тұндыру параметрлерімен (жұмыс газының қысымы, төсемдегі ығысу потенциалы) тығыз байланысты екендігін көрсетті. (Zr-Ti-Cr-Nb-Si)N және (Zr-Ti-Nb)N көпкомпонентті жабындар қарапайым қыры бойынша ортақтандырылған текше (КБТ) қатты ерітінді екендігі анықталды. Құрамында Si жоқ жабындар құрылымы негізінен TiN (КБТ) фаза мен Cr₂N тригоналды модификациядан тұрады. Беріктілік мәндері (24–45 GPa) диапазонда болды. (Zr-Ti-Nb)N және (Zr-Ti-Cr-Nb)N жабындары әртүрлі үйкеліс жағдайында ең ұтымды адгезиялық беріктілікті қамтамасыз етеді. (Zr-Ti-Cr-Nb-Si)N жабындарының адгезиялық беріктіліктің ең төмен көрсеткішке ие болуын салыстырмалы төмен беріктілікпен түсіндіруге болады.

Берілген жабындарды үйкелу жұптар мен кесу құралдарының қорғаныш материалдары ретінде қолдануға болады.

Кілт сөздер: нитридтер, вакуумдық тұндыру, беріктік, адгезия, микроқұрылым, қорғаныш материалдар.

Д.К. Ескермесов, С.А. Пазылбек, А.К. Тусупбекова

Механические и трибологические характеристики многокомпонентных нитридных покрытий на основе Zr, Ti, Nb, Cr и Si

Методом вакуумно-дугового осаждения из многоэлементных катодов Zr-Ti-Nb, Zr-Ti-Cr-Nb и Zr-Ti-Cr-Nb-Si в среде азота (N_2) получены многокомпонентные нитридные покрытия на основе (Zr-Ti-Nb)N, (Zr-Ti-Cr-Nb)N и (Zr-Ti-Cr-Nb-Si)N. Исследования показывают, что химический состав, микроструктура и механические и трибологические свойства покрытий тесно связаны с параметрами осаждения, в частности как: давление рабочего газа и потенциал смещения на подложке. Определено, что многокомпонентные покрытия (Zr-Ti-Cr-Nb-Si)N и (Zr-Ti-Nb)N являются простым гранецентрированным кубическим (ГЦК) твердым раствором. Для покрытий без Si структура в основном состоит из фазы TiN (ГЦК) и тригональной модификации Cr_2N . Значения твердости были в диапазоне (24–45 GPa). Покрытия (Zr-Ti-Nb)N и (Zr-Ti-Cr-Nb)N обеспечивают наилучшую адгезионную прочность в различных условиях трения. Покрытия (Zr-Ti-Cr-Nb-Si)N демонстрировали наихудшую адгезионную прочность, что можно объяснить относительно низкой твердостью. Данные покрытия представляются перспективными в качестве защитных покрытий для пар трения и режущего инструмента.

Ключевые слова: нитриды, вакуумное осаждение, твердость, адгезия, микроструктура, защитные покрытия.